Elastic-instability–enabled locomotion

Amit Nagarkar[a,1], Won-Kyu Lee[a,1], Daniel J. Preston[a], Markus P. Nemitz[a], Nan-Nan Deng[a], George M. Whitesides[a,b,c,2], and L. Mahadevan[c,d,e,f,2]

[a]Department of Chemistry and Chemical Biology, Harvard University, Cambridge, MA 02138; [b]Wyss Institute for Biologically Inspired Engineering, Harvard University, Cambridge, MA 02138; [c]Kavli Institute for Bionano Science and Technology, Harvard University, Cambridge, MA 02138; [d]School of Engineering and Applied Sciences, Harvard University, Cambridge, MA 02138; [e]Department of Physics, Harvard University, Cambridge, MA 02138 and [f]Department of Organismic and Evolutionary Biology, Harvard University, Cambridge, MA 02138

Edited by John A. Rogers, Northwestern University, Evanston, IL, and approved January 5, 2021 (received for review July 8, 2020)

Locomotion of an organism interacting with an environment is the consequence of a symmetry-breaking action in space-time. Here we show a minimal instantiation of this principle using a thin circular sheet, actuated symmetrically by a pneumatic source, using pressure to change shape nonlinearly via a spontaneous buckling instability. This leads to a polarized, bilaterally symmetric cone that can walk on land and swim in water. In either mode of locomotion, the emergence of shape asymmetry in the sheet leads to an asymmetric interaction with the environment that generates movement—via anisotropic friction on land, and via directed inertial forces in water. Scaling laws for the speed of the sheet of the actuator as a function of its size, shape, and the frequency of actuation are consistent with our observations. The presence of easily controllable reversible modes of buckling deformation further allows for a change in the direction of locomotion in open arenas and the ability to squeeze through confined environments—both of which we demonstrate using simple experiments. Our simple approach of harnessing elastic instabilities in soft structures to drive locomotion enables the design of novel shape-changing robots and other bioinspired machines at multiple scales.

elastic instability | locomotion | buckling

Autonomous locomotion in animals enables complex behaviors motivated by the ability to respond dynamically to other animals and to the environment (1). The evolution of locomotion was thus an important step in the history of life, with multiple solutions that were both enabled and constrained by geometry, physics, and biology (2). Many studies of locomotion focus on the neural circuits or mechanisms associated with the active sensing and control of the organism's sense of self and its interaction with the world. However, since directional movement requires the breaking of space-time symmetry associated with the interactions of an organism and its environment (3–5), a physical perspective will complement the current emphasis on the underlying neurobiological processes (6).

Early multicellular organisms were soft-bodied aggregates of cells and polymer matrices that took the form of low-dimensional geometries such as filaments and sheets (7), and were thus easily susceptible to spontaneous symmetry breaking via mechanical instabilities (8). Inspired by this observation, we ask: Might it be possible to harness instabilities to engineer locomotion in a simple physical setting? Such simple locomotors could find use in a range of applications on a range of scales since the basic principle underlying their operation is independent of absolute scale and relies instead on scale separation.

In addition to the choice of geometry, locomotor systems also require design choices that need to be made associated with the choice of the material, a power source required for actuation, control, and sensing, and finally an operating environment. Among the vast array of choices available for each of these subsystems, as shown in Fig. 1 and *SI Appendix*, Figs. S1–S4, we chose a thin axisymmetric circular sheet (thickness t, diameter d) made of a flexible material (modulus E), susceptible to a buckling instability as the symmetry-breaking mechanism, driven and controlled using an oscillatory pneumatic input that is amphibious, i.e., it can operate in both terrestrial and aquatic environments.

When a free circular sheet buckles under the influence of axisymmetric forces out of the plane, it forms an asymmetric developable cone, a singular structure that is the basic constituent of a crumpled sheet, with a shape and response that is well-studied (9–11). Since the buckling stress scales as Et^2/d^2 (9–11), this elastic instability is relatively easy to induce using a pneumatic actuator (*SI Appendix*, Fig. S5). Generating large-amplitude motions is equally easy geometrically with thin sheets because the amplitude scales linearly with disk size for a given cone angle. Similarly, since the asymmetric cone breaks rotational symmetry but is bilaterally symmetric, orienting the direction of locomotion follows naturally. Together, these features allow for gait controllability in an engineered locomotor system.

We use a pneumatic ring actuator attached to thin circular disk made of a flexible polymeric sheet that spontaneously buckles when the pressure inside the ring exceeds a critical value. The symmetric sheet deforms into a bilaterally symmetric polar object, an asymmetric cone with a single invagination that is partly convex and partly concave. When the pressure is released, the sheet recovers its planar shape; however, the next time it is deformed, it deforms the same way due to the small crescent-shaped plastically deformed zone at the center of the cone that provides a geometric memory of the deformation response (9–11). To obtain directed locomotion using this structure requires a mechanism for rectifying this oscillatory response to an oscillatory pneumatic stimulus.

Significance

Soft structures and materials are easily susceptible to mechanical instabilities, which can be harnessed for function, such as controlled locomotion. Here, we show how a reversible conical buckling instability of a pneumatically actuated sheet leads to an amphibious morph-bot that can crawl on land or swim in water. Our approach enables the design of novel shape-changing robots and other bioinspired machines at multiple scales using simple constituent materials and power sources.

Author contributions: A.N., W.-K.L., G.M.W., and L.M. designed research; A.N., W.-K.L., D.J.P., M.P.N., N.-N.D., and L.M. performed research; A.N., W.-K.L., and L.M. contributed new reagents/analytic tools; A.N., W.-K.L., G.M.W., and L.M. analyzed data; and A.N., W.-K.L., G.M.W., and L.M. wrote the paper.

Competing interest statement: G.M.W. acknowledges an equity interest in and board position with Soft Robotics, Inc.; the work described here has no current impact on practical soft robots and actuators.

This article is a PNAS Direct Submission.

[1]A.N. and W.-K.L. contributed equally to this work.

[2]To whom correspondence may be addressed. Email: gwhitesides@gmwgroup.harvard.edu or lmahadev@g.harvard.edu.

This article contains supporting information online at https://www.pnas.org/lookup/suppl/doi:10.1073/pnas.2013801118/-/DCSupplemental.

Published February 18, 2021.

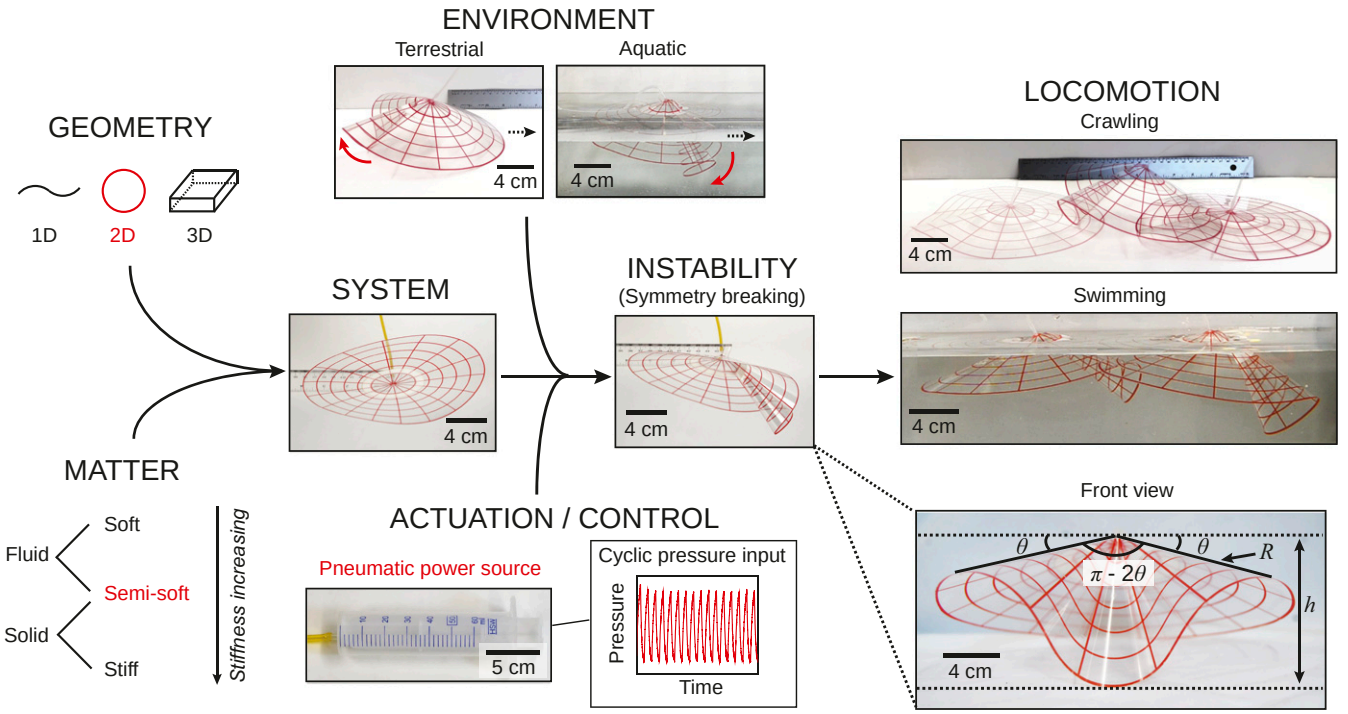

Fig. 1. Schematic representation of the choices of variables available to engineer locomotion. Geometry and material choices make up a system that uses a power source and, on interaction with the environment, causes symmetry breaking, leading to a net directional movement. Buckling of a thin circular sheet is one of the simplest mechanisms of symmetry breaking of an axisymmetric system.

If the buckled conical sheet is in contact with a rough surface, the (rear) concave edge meets the surface at an acute contact angle ($\theta_c < \pi^c/2$), while the (front) convex edge meets it at an obtuse contact angle ($\theta_c > \pi^c/2$), while the wings of the structure are not in contact with the substrate (Fig. 2*A*). The two feetlike contacts of the conical structure with different contact angles leads to a fore–aft frictional asymmetry in the cone's interaction even with a homogeneous substrate; it can slide more easily forward than backward because the concave (rear) foot digs into the substrate more strongly than the convex (front) foot. Furthermore the (front) convex edge can move more easily backward, while the (rear) concave edge can move more easily forward, because of the different tendency of each edge to dig in to the substrate as a function of the contact angle. Thus, when the cone is pneumatically actuated, the (front) convex foot moves forward while the (rear) concave foot remains stuck, and when the pressure is released, the (rear) concave region remains pinned while the (front) convex region slips forward. If the

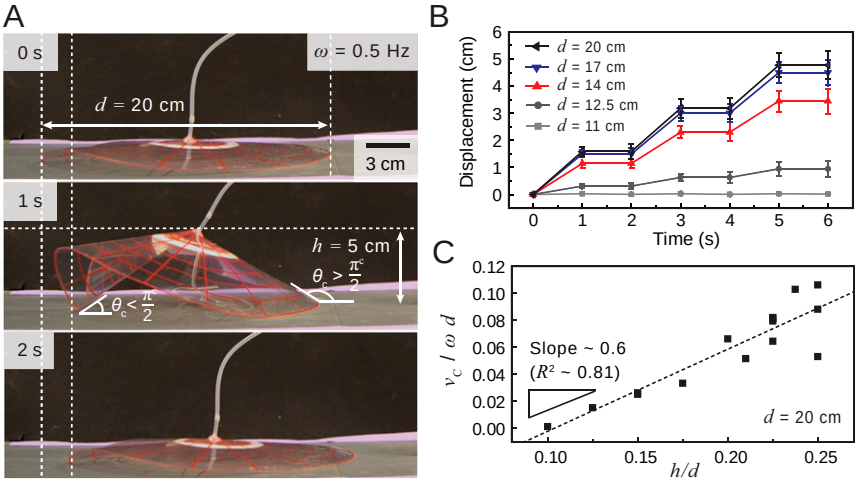

Fig. 2. Locomotion of buckling-sheet actuator with scaling law in terrestrial environment. (*A*) Photos of crawling motion of the buckling-sheet actuator with $d = 20$ cm on a rough surface. (*B*) Displacement vs. time plot for crawling of the buckling-sheet actuator with different d values for $\omega = 0.5$ Hz. (*C*) $v_c/(\omega\, d)$ vs. h plot to show the scaling law for crawling with $d = 20$ cm. The coefficient (slope of linear fit) is ~0.6 ($R^2 \sim 0.81$). All measurements were performed with pneumatic input for buckling of the sheet and vacuum for unbuckling of the sheet. θ_c in *A* is the contact angle between the "foot" of the conimal and the surface.

actuation and release are temporally symmetric with a frequency ω, and the angle of the (symmetric) cone within which the asymmetric cone fits is θ, the average speed of crawling v_c should follow the simple scaling law

$$v_c \sim \omega d\theta \ . \qquad [1]$$

We note that this mode of motion is driven by the geometry-induced asymmetric interaction with the surface, and the speed is limited by the process requiring the longest time (lowest frequency) in the system.

If the sheet is submerged in water (density ρ) and deformed into a polar cone, it displaces water. In the limit when viscous forces dominate, i.e., when the Reynolds number $Re << 1$, when the cone reverts to a sheet, the water is again displaced, but in the opposite sense, and thus the sheet does not undergo any net movement. However, if we break symmetry in time by deforming rapidly over the first half-cycle and slowly over the second half, such that at least one motion occurs with $Re \geqq 1$, we see net motion. This type of unsteady motion is similar to that seen in medusoids, such as jellyfish (12). The average force due to pressure drag scales as $F_d \sim \rho v_s^2 d^2 f(Re)$ while the average propulsive force to accelerate a fluid bolus of volume $d^3\theta$ to average speed v_s ~scales as $F_p \sim \rho d^3\ \theta v_s \Delta\omega$, where $\Delta\omega = \omega_B - \omega_U$, is the difference in the rate of forming a cone (bending) and relaxing back to a sheet (unbending). Balancing the two yields an expression for the speed

$$v_s \sim \Delta\omega d\theta / f(Re), \qquad [2]$$

where the function $f(Re)$ can only be calculated numerically by solving the complete elastohydrodynamic problem. Here, we note that the speed is controlled by the temporal asymmetry associated with bending and unbending the soft sheet. The similarity between [**1**] and [**2**] is a natural consequence of the fact that in both cases, spontaneous symmetry breaking leads to the formation of soft polar objects that interact asymmetrically with their environments and thus move. However, locomotion in a fluid requires breaking time-reversal symmetry, a well-known requirement (13), while the geometry of the cone automatically provides asymmetric frictional interactions when moving on a rough substrate.

To test these predictions, the conical sheet actuators were first placed on a rough surface and actuated with an oscillatory pneumatic input of variable frequency and amplitude. We see that the oscillatory pneumatic input leads to periodic buckling and thence net translational movement on a rough surface (Fig. 2*A*). We systematically studied the dependence of the crawling velocity of the locomotion with the diameter of the disk (d), the maximum height of the buckle (h, noting that $h \sim d\theta$), which is easier to visualize, and the frequency (ω) of actuation (Fig. 2*B* and *SI Appendix*, Figs. S6 and S7). Here, we defined $\omega = 1/t_T$, where $t_T = t_B + t_U$ (t_T is the period of one buckling–unbuckling cycle, t_B is the buckling time, and t_U is unbuckling time, respectively). For all the crawling experiments, we used pneumatic input for buckling of the sheet and vacuum for unbuckling of the sheet such that $\omega_B = \omega_U$. We see that our experiments agree with the scaling law [**1**], as indicated in Fig. 2*C*, with an experimentally measured prefactor that is 0.6, so that $v_c \cong 0.6\omega d\theta$. The discrepancies at large values of h are likely due to the heterogeneity of the frictional interaction with the surface.

We then investigated the ability to harness this instability to generate net directional movement in an aquatic environment (Fig. 3*A*). Periodic buckling against viscous forces leads to a swimming motion only when the active buckling frequency $\omega_B = 1/t_B$ is larger than active unbuckling frequency $\omega_U = 1/t_U$, and we independently tuned ω_B and ω_U using electronic control devices for the motions (*SI Appendix*, Fig. S3). We investigated the dependence of the swimming velocity by varying d, h, and ($\omega_B - \omega_U$) (Fig. 3*B* and *SI Appendix*, Fig. S8). The buckling frequency was kept constant ω_B of ~0.83 Hz, the unbuckling frequency ω_U was varied between 0.3 and 0.83 Hz, and the size of the sheet was varied between 12 and 20 cm. Fig. 3*C* shows that the proposed scaling law [**2**] is valid for aquatic locomotion. In this case, as unbuckling is the rate-determining step, the velocity of swimming v_S scales linearly with the frequency difference ($\Delta\omega = \omega_B - \omega_U$), and the experimentally measured prefactor for the scaling law [**2**] is ~0.5, comparable with that of crawling motion for the range of

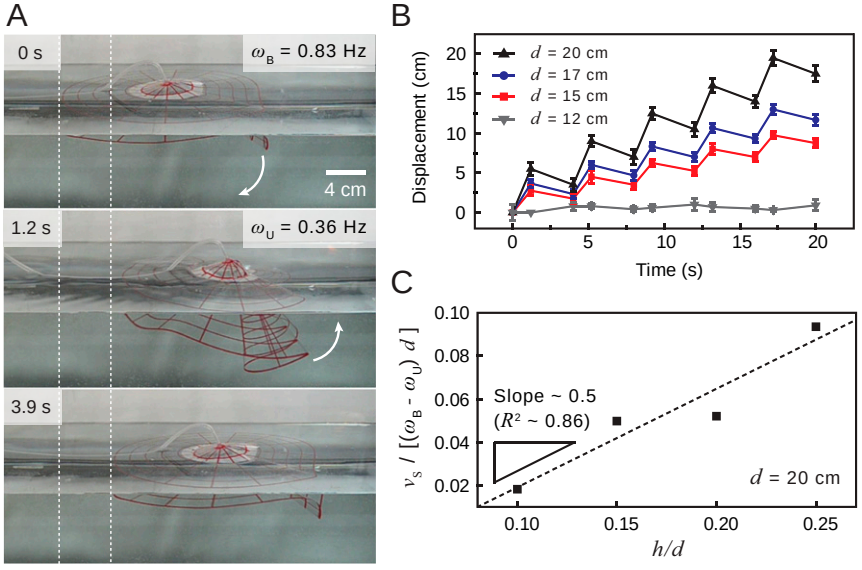

Fig. 3. Locomotion of buckling-sheet actuator in aquatic environment. For swimming motion, the actuator with different diameters (d) was actuated with a constant buckling frequency (ω_B) and varying unbuckling frequency (ω_U). (*A*) Photos of buckling-sheet actuator with d = 20 cm swimming on the surface of water. The actuator moves only when the buckling frequency (ω_B) is larger than the unbuckling frequency (ω_U). (*B*) Displacement vs. time plot for swimming of the buckling-sheet actuator with different d values for $\omega_B \sim 0.83$ Hz and $\omega_R \sim 0.36$ Hz. (*C*) The plot of the scaling law for swimming, $v_S/[(\omega_B - \omega_U)\ d)]$ vs. h/d with d = 20 cm. The coefficient (slope of linear fit) is ~0.5 ($R^2 \sim 0.86$).

actuation frequencies we use. It is worth pointing out that the direction of motion in an aquatic environment is exactly opposite that on land, as the fold is a pusher on land and a puller in water. This implies that in a littoral zone, this "con(e-an)imal" will remain localized, going back and forth between land and water.

Our engineered system shows how a minimal symmetry-breaking mechanism in a soft sheet suffices to generate locomotion in both terrestrial and aquatic environments. To make the two gaits successful and functional, though, we need to address the question of their efficiency—that is, the ratio of the physical work they perform during locomotion versus the input energy required (13, 14)—and their controllability. In both engineered and evolved systems, the efficiency of locomotion determines whether a design is successful or not. Here, locomotion arises from actively driving the system only over half the cycle and while allowing the system to recover passively over the other half (*SI Appendix*, Fig. S9). In our experiments so far, the orientation of the polar cone is random and determined by the spontaneous breaking of rotational symmetry induced by buckling. To control the direction of locomotion we use two actuators on a pair of mechanically coupled sheets with separate pneumatic inputs (*SI Appendix*, Fig. S10) that are now designed to be polar. Actuating either of the two buckles independently leads to turning motion, while actuating both buckles simultaneously leads to linear translational motion (*SI Appendix*, Fig. S10). We can also take advantage of the softness of the sheet to change its shape dynamically and thus squeeze through a narrow opening with a footprint that is smaller than that of the extended flat sheet (*SI Appendix*, Fig. S11). Furthermore, the conimal can achieve jellyfishlike motion in water by squirting water jets as it buckles, mimicking simple soft-bodied jellyfishlike organisms (*SI Appendix*, Fig. S12). Finally, it is also noteworthy that the buckling-sheet actuator driven by elastic instabilities can perform untethered locomotion with an integrated electropneumatic source (*SI Appendix*, Fig. S13) as well as display real-world applications such as a robotic gripper (*SI Appendix*, Fig. S14).

Our choices of geometry and actuation have yielded a polar, bilaterally symmetric morphology that arises naturally from a static elastic instability and enables stable and robust amphibious locomotion using relatively simple materials and power sources. The purely geometric instability to generate locomotion is time-independent, complementing other systems that rely on dynamic bistability associated with snapping behavior (15–17), and marks the beginning of an exploration of other forms of morphological phenotypes that serve as primitives for soft robotic locomotion (18, 19). In a biological context, perhaps it might not have been too difficult to harness this soft mode of deformation to effect directed movement in benthic environments, and thus enable the evolution of locomotion in primitive soft-bodied multicellular organisms, setting off a cascade whose consequences we now see around us (1).

Data Availability. All study data are included in the article and/or supporting information.

ACKNOWLEDGMENTS. This research was funded by the Department of Energy, Office of Basic Energy Science, Division of Materials Science and Engineering, under Award ER45852, which funded all work related to experimental apparatus and demonstrations. A.N. acknowledges partial salary support from Defense Advanced Research Projects Agency (DARPA) Award W911NF-18-2-0030. L.M. acknowledges support from the following grants: NSF DMR 20-11754, NSF DMREF 19-22321, and NSF EFRI 18-30901.

1. M. Wilkinson, *Restless Creatures: The Story of Life in Ten Movements* (Basic Books, New York, 2016).
2. M. H. Dickinson *et al*., How animals move: An integrative view. *Science* **288**, 100–106 (2000).
3. J. Gray, *Animal Locomotion* (Weidenfeld and Nicolson, 1968).
4. M. F. Glaessner, *The Dawn of Animal Life: A Biohistorical Study* (Cambridge University Press, 1984).
5. J. J. Collins, I. N. Stewart, Coupled nonlinear oscillators and the symmetries of animal gaits. *J. Nonlinear Sci.* **3**, 349–392 (1993).
6. E. D. Tytell, P. Holmes, A. H. Cohen, Spikes alone do not behavior make: Why neuroscience needs biomechanics. *Curr. Opin. Neurobiol.* **21**, 816–822 (2011).
7. R. B. Clark, *Dynamics of Metazoan Evolution* (Cambridge University Press, 1968).
8. L. Mahadevan, S. Daniel, M. K. Chaudhury, Biomimetic ratcheting motion of a soft, slender, sessile gel. *Proc. Natl. Acad. Sci. U.S.A.* **101**, 23–26 (2004).
9. E. Cerda, S. Chaieb, F. Melo, L. Mahadevan, Conical dislocations in crumpling. *Nature* **401**, 46–49 (1999).
10. E. Cerda, L. Mahadevan, Conical surfaces and crescent singularities in crumpled sheets. *Phys. Rev. Lett.* **80**, 2358–2361 (1998).
11. E. Cerda, L. Mahadevan, Confined developable elastic surfaces: Cylinders, cones and the Elastica. *Proc. R. Soc. A* **461**, 671–700 (2005).
12. R. M. Alexander, *Mechanics of Animal Locomotion* (Cambridge University Press, 1992).
13. E. R. Weibel, C. R. Taylor, L. Bolis, Principles of animal design: The optimization and symmorphosis debate. *Q Rev Biol*, 74, 233–234 (1999).
14. R. M. Alexander, Models and the scaling of energy costs for locomotion. *J. Exp. Biol.* **208**, 1645–1652 (2005).
15. Z. Zhakypov, K. Mori, K. Hosoda, J. Paik, Designing minimal and scalable insect-inspired multi-locomotion millirobots. *Nature* **571**, 381–386 (2019).
16. L. Meng *et al*., A mechanically intelligent crawling robot driven by shape memory alloy and compliant bistable mechanism. *J. Mech. Robot.* **12**, 061005 (2019).
17. S. W. Kim, J.-S. Koh, M. Cho, K.-J. Cho, "Towards a bio-mimetic flytrap robot based on a snap-through mechanism" in *2010 3rd IEEE RAS & EMBS International Conference on Biomedical Robotics and Biomechatronics* (Institute of Electrical and Electronics Engineers, Tokyo, 2010), pp. 534–539.
18. R. Pfeifer, M. Lungarella, F. Lida, The challenges ahead for bio-inspired 'soft' robotics. *Commun. ACM* **55**, 76–87 (2012).
19. G. M. Whitesides, Soft robotics. *Angew. Chem. Int. Ed. Engl.* **57**, 4258–4273 (2018).